PHYSICAL CHARACTERISTICS OF COMETARY DUST FROM OPTICAL STUDIES

Martha S. Hanner
Jet Propulsion Laboratory

Observations of the scattered sunlight and thermal emission from cometary dust provide information on the composition and dominant size of the dust. The observations will be summarized here and compared to theoretical models for dielectric and absorbing materials, with emphasis on the thermal emission. The compatibility of the optical data with the size distribution derived from dynamical studies is discussed.

Comets are considered to be the most primitive objects in the solar system; they contain the clearest record of the undifferentiated material from which the solar system formed [1]. In addition, comets are the most probable source of the present interplanetary dust cloud. The composition and size distribution of the solid grains released from comets give information on the composition of the comet nucleus, the physical processes of cometary disintegration, and the "source function" for the interplanetary dust cloud.

Optical observations of the continuum radiation from comets can be used to infer the physical properties of the dust grains. The relevant data consist of brightness and polarization measurements of the sunlight scattered by the dust particles as a function of scattering angle and wavelength and measurements of the infrared thermal emission from the dust as a function of heliocentric distance (and hence grain temperature). In this paper, I will summarize the available optical observations and discuss the general nature of the dust grains which can be inferred from these data.

The wavelength dependence of the scattered light is an indicator of the size of the scattering particles. Observations in the near-infrared show that the color of the coma matches the solar spectrum from 1 μm to 1.65 μm for the 4 comets measured: Bennett [2], Kohoutek [2, 3], Bradfield [2,4], and West [5, 6]. Wavelength independent scattering can result if λ is beyond the peak in the scattering coefficient. For non-absorbing silicates, this implies particle diameter $\gtrsim$ 2 μm; for somewhat absorbing material a diameter $\gtrsim$ 1 μm.

223

The color of the continuum radiation from the coma in the visible part of the spectrum is unclear. Observations range from neutral to considerably reddened. Gebel measured a constant brightness relative to the sun between .35 µm and .65 µm from spectrophotometry of Comets 1967n and 1968c. [7]. Stokes concluded that the coma of Comet Bennett was redder than the Sun from photographic spectrophotometry between .45 µm and .8 µm. He found a brightness increase relative to the sun of 30% from .6 µm to .8 µm [8]. Johnson et al., using interference filters, detected only slight reddening in Bennett, a 10% increase in comet/sun brightness from 0.4 µm to 1.1 µm [9]. Babu measured a color change in Comet Kohoutek from G8 III on 12/7 to solar color (G2V) on 12/15 in the .37 µm to .64 µm region [10]. Ney reported approximately solar color in VRI bandpasses for both Bennett and Kohoutek, as well as Bradfield and West [2, 5]. The problem with all of these measurements is the separation of continuum from emission features. Certainly the V bandpass includes strong C_2 bands. It is not clear whether the continuum is reached between bands in the .73µm-.83µm region. There are numerous CN bands, as well as NH_2 and H_2O^+ although they are relatively weak in dusty comets. At least part of the differences in the observed colors may be real and may indicate variations in the size distribution and perhaps the physical nature of the grains. A'Hearn et al have suggested that the color is correlated with gas/dust ratio, being bluer than the Sun in dust-poor comets, including P/Encke [11]. Combined measurements of color and polarization for the same volume of dust would be more useful than color alone for determining grain properties.

The dust tail is composed of particles which have been influenced by radiation pressure and, depending on the viewing geometry, will have a size distribution which differs from that in the coma. Liller found a reddening $\propto \lambda^2$ from spectrophotometry of the tails of Comets Arend-Roland (1956h) and Mrkos (1957d), which he fit by iron spheres of radius 0.3 µm [12]. Donn et al. [13] pointed out that the observed polarization was too low to fit the scattering by iron spheres.

The average scattering function of the dust grains can be obtained by observing the comet coma with changing earth-comet-sun geometry or by scanning along the comet tail. Both methods have the difficulty of separating out any changes in the scattering properties of dust emitted from the nucleus at different times. Most comets have been observed near 90° phase angle. Comet West provided an opportunity to observe the coma over a wide range of angles, since it passed between the earth and sun. Ney has used the ratio of visible to infrared brightness for each day to derive the scattering function from 34° to 150° scattering angle [5]. The shape is consistent with micron-size slightly absorbing dielectric particles or larger irregular particles, as discussed by Giese [14].

The average Bond albedo, A, of the dust grains can be obtained by comparing the visible scattered light to the thermal emission

from the same volume of dust. The albedo is defined as

$$A = \frac{Q_{scat}}{Q_{scat} + Q_{abs}} \qquad (1)$$

$$\frac{A}{1-A} = \frac{Q_{scat}}{Q_{abs}} \qquad (2)$$

Q_{scat}/Q_{abs} is equivalent to the observed scattered radiation at visible wavelength (integrated over scattering angle) divided by the total integrated infrared flux [15]. Albedos derived in this way typically range from 0.1 to 0.4 [15, 16]. Generally, the scattered radiation is assumed to be isotropic. As Ney [5] points out, this assumption, together with observations near 90°, leads to an underestimate of the albedo. For Comet West, Ney derives A = 0.3-0.5, depending on the estimated shape of the scattering function outside the range 34°-150°; the single data point near 90° would have led to an albedo of 0.15.

The polarization of the scattered light is an important parameter for defining both the size and physical properties (refractive index, shape, roughness) of the dust grains. Comparison of visible and near-infrared data for the same comet shows no clear wavelength dependence of polarization, indicating particle sizes ≈ 1 µm or larger. Some of the visible light observations are unfortunately wide-band and are probably contaminated by molecular emission, which also exhibits polarization [17]. Blackwell and Willstrop measured the phase angle dependence for the coma of Arend-Roland using a filter centered at .453 µm [18]. Their filter avoids the main molecular features, but may include some contribution from the C_2 band near .47 µm. Polarization varied smoothly from 19.5% at phase angle 62° to 5% at 42°. The phase angle dependence in the near-infrared was measured by Oishi et al [6]. They observed the coma of Comet West at phase angles from 100° to 65°. The maximum polarization was $\approx 30\%$ between 100° and 90°, decreasing to $\approx 20\%$ at 65°. The polarization of Comet West at 90° was somewhat higher than that observed by Noguchi et al [3] for Kohoutek at the same wavelengths and phase angle.

As the history of zodiacal light interpretation has showed us, polarization by itself can be interpreted in a number of ways. A major contribution from submicron grains is ruled out by the near-infrared color. Oishi et al proposed that the polarization arises from a mixture of micron-size metallic and silicate particles, which also produce the infrared thermal emission [19].

Ono suggested Fresnel reflection from irregular particles [20]. Laboratory experiments have shown that larger irregular absorbing particles could also explain the polarization [14].

Maps of the direction and degree of polarization in the coma have been made by Clarke [21] for Comet Bennett and Isobe et al [22] for Comet West after the nucleus had split. Both maps show considerable spatial structure within the coma, with polarization ranging from a few per cent to well over 20%. Both maps also show regions of negative polarization, where the maximum E vector was parallel to the scattering plane. These variations may be explainable by spatial variation in particle size resulting from radiation pressure or, particularly for Comet West which had recently split into 4 nuclei, change in the predominant particle size emitted from the nucleus. Unfortunately, both maps were wide-band observations, which included the strong C_2 emission bands. Although Bennett and West were dusty comets, some contamination from emission is probably present and may contribute to the observed spatial variations.

The most interesting polarimetric observations are by Weinberg and Beeson, who scanned along the tail of Comet Ikeya-Seki through a series of narrow-band filters [23,24]. The polarization at .53 μm varied from +20% to -40% over a $20°$ range in phase angle. The neutral point varied from $\theta = 58°$ to $48°$ in 7 days and also varied with wavelength. A likely explanation of these data is a variation of particle size with position along the tail. Many kinds of particles have a transition from positive to negative polarization for radius slightly larger than 0.1 μm at these phase angles [25]. In particular, silicate particles exhibit strong negative polarization for a range of particle sizes a > 0.1 μm. Krishna Swamy concluded that slightly absorbing silicates, m = 1.65 - 0.05 i, could exhibit the expected behavior and be consistent with the dynamics [25].

Infrared thermal emission from the dust provides independent information on the properties of the dust particles. The grain temperature, as a function of solar distance, varies with both particle size and composition. The spectral energy distribution also is an indicator of particle size and composition. Since the first infrared observations of Ikeya-Seki by Becklin and Westphal [26], all of the bright comets have been observed in the infrared between 1 μm and 20 μm [2-6, 27-33]. The infrared emission has the following general characteristics: solar spectrum λ < 1.65 μm; 3 μm - 5 μm color temperature $\geq$ black body; broad feature 8 μm - 13 μm; emission feature near 18 μm.

The most extensive observations have been carried out by Ney, using a series of broad bandpass filters, $\lambda/\Delta\lambda \sim 10$ [2]. Figure 1a, taken from Ney, illustrates the infrared emission for Comet Kohoutek, pre-perihelion and Comet Bennett, post-perihelion at the same heliocentric distance. The 3.5 μm - 4.8 μm color temperature for Bennett is 518 K, and for Kohoutek 440 K, whereas the blackbody temperature at this heliocentric distance is only 350 K. The 10 μm and 18 μm features are stronger in Bennett, relative to a blackbody curve fit at 3.5 μm to 4.8 μm; the ratio of 10 μm to 3.5 μm brightness is actually the same in both comets in Figure 1a.
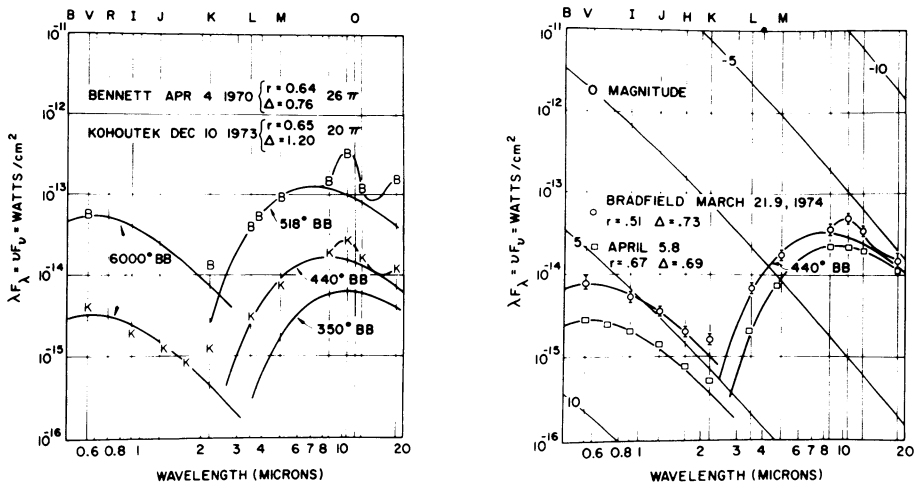
Fig. 1. Energy spectra of recent comets [2]. 1a. Bennett vs. Kohoutek at 0.64 AU. 1b. Disappearance of 10 μm feature in Bradfield.

The 8 μm – 13 μm region in Kohoutek was scanned by Merrill [32]. These data show a broad, structureless feature similar to that observed in interstellar sources, with a maximum near 9.6 μm. The strength of the 10 μm emission relative to the continuum varies from one comet to another and with time in the same comet. The feature disappeared in Bradfield between March 21 (r = 0.51 AU) and April 5 (r = 0.67 AU) as illustrated in Figure 1b [2]. Comet Kobayashi-Berger-Milon did not show any 10 μm excess above a blackbody continuum [33]. The 10 μm and 18 μm peaks are generally attributed to silicate particles, although formaldehyde polymers have been suggested [34,35]. The presence of the peaks sets an upper limit of a few microns on the size of the emitting grains.

To illustrate the thermal properties of dust grains, I will present models based on two types of grain materials: magnetite, a typical absorbing material found in the micrometeoroids collected by Brownlee [36] and olivine, an iron-magnesium silicate also seen in collected micrometeoroids and in carbonaceous chondrites. The refractive index for magnetite is from Huffman and Stapp [37]. The refractive index for olivine, 8 μm – 24 μm, is from measurements by Krätschmer and Huffman for a disordered olivine sample [38,39], extended to 35 μm by Huffman (personal communication) based on an oscillator model. Three values for the absorption at visible wavelengths were used, k_v = 0.001, 0.01, 0.04, to illustrate the thermal properties of a slightly absorbing material.

In order to compare the optical results with dynamical studies, I have used the size distribution derived for Comet Bennett from dynamical analysis [40,41], modified for the large particles to agree with the dynamical analysis of comet anti-tails [42]:

$$n(a) = 0 \qquad\qquad\qquad 2a\rho < 0.9 \times 10^{-4} \, cm$$

$$n(a) = \frac{0.69 \ (2a\rho - 0.9 \times 10^{-4})}{(2a\rho)^5} \qquad 0.9 \times 10^{-4} \le 2a\rho \le 2.6 \times 10^{-4} \, cm$$

$$n(a) = 0.08656 \ (2a\rho)^{-4.2} \qquad 2\rho a > 2.6 \times 10^{-4} \, cm$$

where a = radius (cm) and ρ = particle density (gm/cm^3). I have used this size distribution in two forms, one with $\rho = 1 \, gm/cm^3$, $a_{min} = 0.45 \, \mu m$ (SM1), the other with $\rho = 2.6 \, gm/cm^3$, $a_{min} = 0.17 \, \mu m$ (SM2).

The size distribution is derived by comparing the particle trajectories as a function of β with the brightness isophotes, where

$$\beta = F_{rad}/F_{grav} = const. \ Q_{pr}/\rho a. \qquad\qquad (3)$$

Q_{pr} is the efficiency factor for radiation pressure. The size distribution for Bennett was derived assuming $Q_{pr} = 3/2$, independent of grain size. Figure 2a illustrates the variation of Q_{pr} with grain radius computed from Mie theory for the magnetite and olivine. $Q_{pr} = 3/2$ is close to the value for magnetite, $a \approx 1 \, \mu m$, but is high for the olivine. The explicit form for n(a), including Q_{pr}, is given in [43].
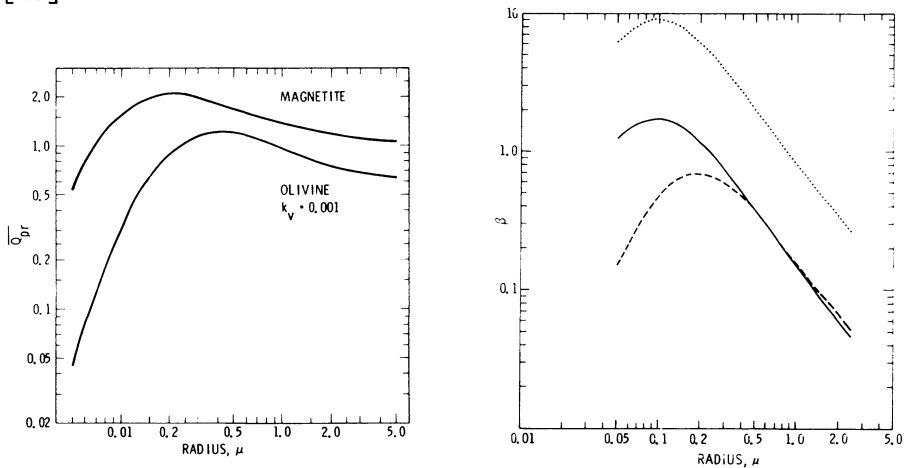

Fig. 2a. $\overline{Q_{pr}} = \int Q_{pr} S_\lambda d\lambda / \ S_\lambda d\lambda$ vs. particle radius (Mie theory). 2b. $\beta = F_{rad}/F_{grav}$ vs. particle radius.——magnetite,--- olivine,...magnetite $\rho = 1$.

The variation of β with grain radius is shown in Figure 2b. Olivine has $\beta_{max} = 0.65$, typical of dielectric material. Magnetite, with $\rho = 5.18 \, gm/cm^3$ has $\beta_{max} = 1.75$. Since F_{rad} is proportional to surface area, while F_{grav} depends on total mass, a porous, fluffy absorbing particle can be expected to have a higher β than a sphere, illustrated qualitatively by the dotted curve for magnetite with
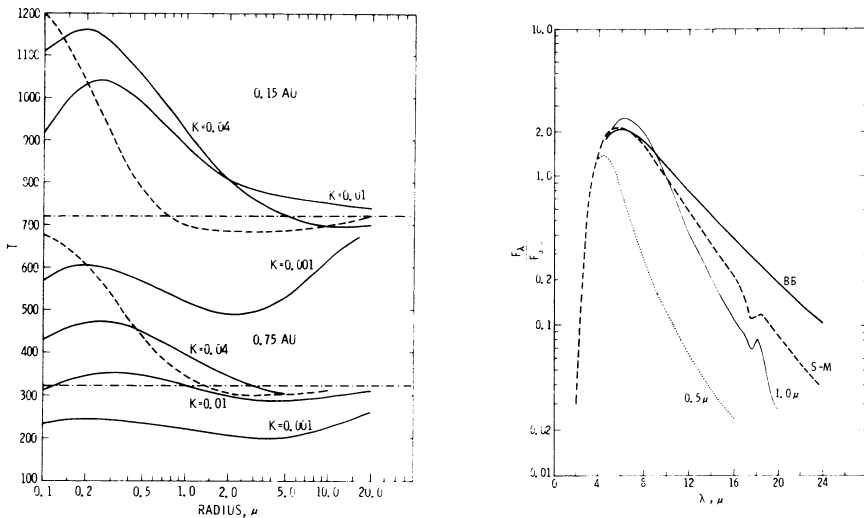
Fig. 3. Thermal properties of grains. 3a. Temperature vs. radius---magnetite,——olivine,-·-·black body. 3b. Emission vs. λ for magnetite grains at 500 K. ...a = 0.5 μm,——a = 1.0 μm, ---SM1,——black body

$\rho = 1$ gm/cm^3. This may be an explanation for the striae analyzed by Sekanina in Comet West [44]. He concluded that the parent particles, (a > 1 μm) had β > 1 before fragmentation.

Grain temperatures as a function of size and heliocentric distance were computed by equating the total energy absorbed to the total energy emitted.

$$\pi a^2 \left(\frac{R_O}{R}\right)^2 \int Q_{abs}\ S_\lambda\ d\lambda = 4\pi a^2 \int \pi B_\lambda(T)\ Q_{abs}\ d\lambda \qquad (4)$$

where S_λ = solar flux from Labs and Neckel [45]; Q_{abs} = absorption efficiency factor computed from Mie theory; $B_\lambda(T)$ = Planck function at temperature T. Figure 3a shows the grain temperature vs. size for 2 solar distances. Magnetite grains, a ≤ 1 μm are hotter than a black body; these small grains cannot radiate efficiently in the infrared. Olivine, k_v = 0.001, is 100 K or more cooler than a black body for a ≤ 10 μm. Addition of a small absorption raises the grain temperature considerably. Note that grains which approximate the black body temperature at 0.75 AU (k_v = 0.01) are considerably hotter at smaller solar distances, hotter than the magnetite grains, as the peak of the Planck function has shifted away from the middle infrared, where these grains can radiate efficiently.

Figure 3b illustrates that grains of a given temperature can not radiate efficiently at wavelengths ≳ 10 times their radius. Therefore, a black body fit to observed infrared fluxes at 3-6 μm does not
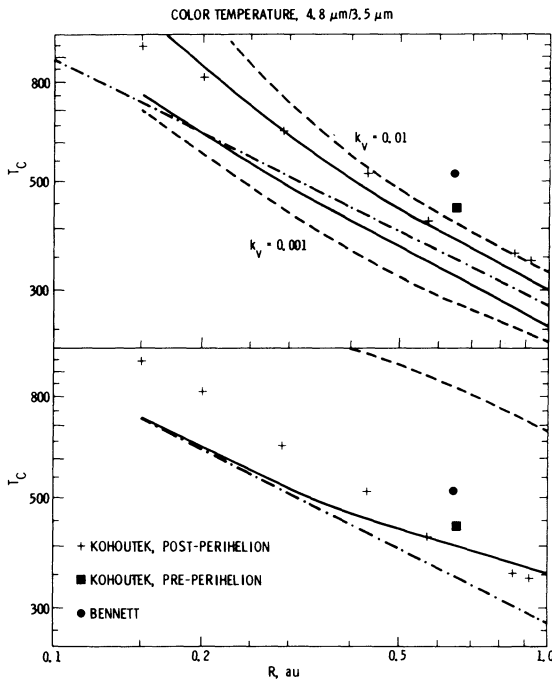
COLOR TEMPERATURE, 4.8 μm/3.5 μm

Fig. 4. Color Temperature vs. Solar Distance. Upper plot: olivine, lower plot: magnetite.——SM1,---SM2,-·-· black body.

necessarily imply a smooth black body continuum at longer wavelengths. A black body continuum out to 18 μm was observed for Bradfield at 0.67 AU (Fig. 1b) and in the anti-tail of Kohoutek [2], indicating that the emitting particles were at least a few microns in diameter. But if the SM size distribution is correct and if the particles are not too porous ($\rho > 1$ gm/cm^3), it is questionable how the continuum should generally be drawn in the presence of the 10 μm and 18 μm features.

To model the color temperatures, the thermal emission at each wavelength was computed and integrated over the particle size distribution, using the appropriate grain temperature for each grain size and heliocentric distance. The 4.8 μm/3.5 μm brightness ratio was used to define a color temperature, for comparison with Ney's data [2]. These color temperatures are plotted in Figure 4. Solid lines refer to SM1, dashed lines to SM2. As expected from Figure 3a, sub-micron absorbing grains (SM2) are far too hot to be compatible with observations. Olivine grains with $k_v = 0.001$ are too cool to match the data. The slightly absorbing olivine, $k_v = 0.01$ and SM1, fits the Kohoutek data. The single data point for Bennett requires somewhat smaller absorbing grains or a "dirtier" silicate. Absorbing grains, a > 1 μm, such as magnetite, are reasonable if one does not place too much emphasis on the high temperatures for Kohoutek at small R. If the grains are too large, the temperature will approach a black body. Mukai [46] and Krishna Swamy & Donn [47] reached similar conclusions from model calculations. Mukai plots color ratio directly, instead of temperature. He concludes that ≈ 1 μm absorbing particles fit the Kohoutek data within the observational errors.

If absorbing grains are the source of the infrared emission, they do not have the size distribution derived for Bennett unless they are very fluffy, $\rho \sim 1$ gm/cm^3. Sekanina derives $\beta_{max} \approx 2$ for Bennett [43],
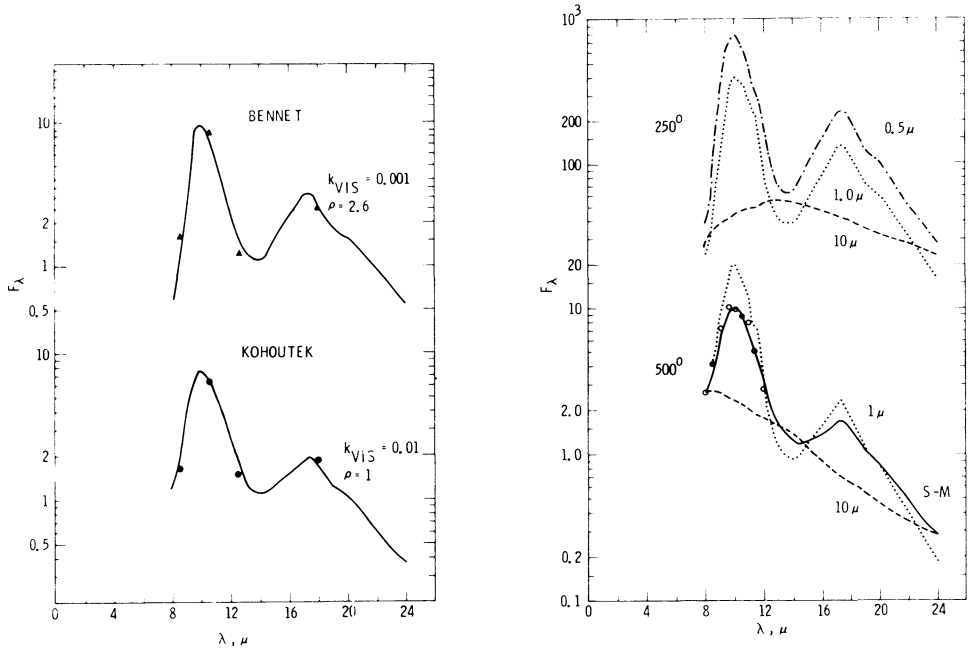
Fig. 5. Silicate Emission Features. 5a. Bennett data, [2] and SM2 model, k_V = 0.001; Kohoutek data, and SM1 model, k_V = 0.01. 5b. Dependence on grain size. ——SM1, oo Kohoutek [32].

which is higher than the β_{max} for slightly absorbing silicates or absorbing grains of high density. Arend-Roland and Seki-Lines, on the other hand, had β_{max} = 0.55 [43], which would suggest a dielectric as the main source of the scattered light, or else an absence of particles with a $\leq$ 0.5 μm.

If the thermal continuum emission can be explained by slightly absorbing silicate grains, can these same grains give rise to the 10 μm and 18 μm emission? Specifically, what is the ratio of 10 μm to 3.5 μm emission predicted by the olivine models, compared to that observed? The answer is given in Table 1 for R = 0.64 AU, SM1. Similar results apply at other solar distances. If these refractive indices are typical — very little absorption in the near infrared and strong absorption at $\geq$ 8 μm, the same particles can not account for both the continuum and 10 μm emission. Krishna Swamy & Donn obtained somewhat better agreement using dielectric constants for a lunar rock sample, but the fit was still not good [47].

Table 1. 10.6 μm/3.5 μm Flux Ratio

k_V=0.001	k_V=0.01	Bennett, 0.65 AU	Kohoutek, 0.64 AU
3100	150	~3	~3

If we then assume two components for the dust, we can examine how well the olivine model will fit the 10 μm and 18 μm emission peaks alone. Figure 5b shows how the shape of the emission features depends on grain size and temperature. Although a feature is no longer visible for a = 10 μm, the emission is still elevated above emission at shorter wavelengths. The spectrophotometric data for Kohoutek at 0.31 AU [32] are plotted in Figure 5b and agree well with the SM1 model.

The computed models are compared with Ney's observations of Bennett and Kohoutek in Figure 5a. The spectrum of Bennett can be fit with k_v = 0.001 and SM2. For Kohoutek, somewhat larger, slightly absorbing grains would give a good match (k_v determines grain temperature). This comparison is not meant to imply uniqueness for a particular model or particular olivine sample, but it does indicate that a disordered or amorphous olivine can give a reasonable representation of the data for appropriate sizes and grain temperatures. As Krätschmer and Huffman point out, the disordered olivine predicts the emission feature near 18 μm, whereas other amorphous silicates have the feature beyond 20 μm. Spectral reflectivity measurements have been made on powdered samples of carbonaceous chondrites. These samples show no feature near 18 μm, but rather a feature near 22 μm and a weaker one at 16 μm [48,49].

Optical observations of recent bright comets, then, lead to the following general characteristics of the dust grains: The optically important particle size is $\approx$1 μm, to be consistent with the solar color from 1 μm to 1.65 μm as well as the 4.8 μm/3.5 μm color temperature. Silicate particles not larger than a few microns are usually (but not always) present; however pure silicate grains can not be responsible for the thermal emission, because of their low equilibrium temperature. The silicate emission can be represented by a disordered olivine; it is not compatible with average carbonaceous chondritic material. The size distribution and β_{max} derived for Comet Bennett from dynamical analysis are not consistent with the size inferred from optical data if the particles are spherical grains of high density.

Measurements beyond 1 μm, which are diagnostic for both size and composition, have been obtained for only a few bright dusty comets and may not be typical of less dusty or short-period comets – or even other dusty comets. Shower meteors associated with different meteor streams have distinct differences in density, for example [50]. Donn compared the gas/dust ratio for 87 comets [51]. He concluded that there are intrinsic differences among comets, which are independent of their evolutionary stage. Kobayashi–Berger–Milon, which showed no 10 μm peak, had a high gas/dust ratio. A'Hearn et. al suspected a correlation of the gas/dust ratio with the color of the scattered light, suggesting a variation in particle size [11]. They measured a blue continuum for 3 dust-poor periodic comets, which would indicate small particles, and a neutral color for P/Chernykh, a periodic comet with perihelion at 2.56 AU and an unusually strong continuum. Variations in β_{max} and mean particle size also suggest intrinsic differences among comets [41].

The cometary dust grains may be conglomerate, irregular particles of varying composition, if the micrometeoroids collected by Brownlee [36] are typical. Appropriate theoretical representation of such particles is a problem for both optical and dynamical interpretations. It would be helpful to have measurements of the optical constants for some of the collected micrometeoroids, including some which contain olivine. The radiation pressure for non-spherical particles needs to be treated. In any event, derivation of a size distribution from f(β) should explicitly take into account the variation of Q_{pr} with size and composition.

Ultimately, physical characteristics of the dust - mineralogy and heterogeneity as well as bulk chemical composition and size distribution - will come from direct sampling of dust during a comet rendezvous mission. Since space probes will only sample one, or possibly a few, periodic comets however, remote sensing remains a valuable tool and the only technique to study the full range of cometary characteristics.

Accurate polarization and color observations in the visible and near-infrared are needed for cometary comae and tails, with good spatial and temporal coverage, through filters which are carefully chosen to exclude emission. Observatories engaged in zodiacal light or airglow research should make particular effort to acquire suitable filters and to observe comets at every opportunity. The polarization versus phase angle can be particularly useful in monitoring changes in particle characteristics, when combined with near-infrared color observations of the same region.

Comets with small perihelion distance serve as probes of the behavior of dust grains at high temperature. Infrared observations of these comets can provide the thermal history of the dust grains. Spectrophotometric scans of the silicate emission features near the sun would be particularly interesting. When laboratory samples of non-crystalline silicate are heated to 1000K, the structure characteristic of crystalline silicate appears in the 10 μm emission [52]. Finally, a clearer understanding of the kind of silicate material present in comets may give clues to the composition of interstellar silicate grains which produce similar 10 μm and 18 μm features.

REFERENCES

1. Delsemme, A.H. 1977, Comets, Asteroids and Meteorites, ed. A.H. Del-semme, Univ. Toledo, pp. 3-13.
2. Ney, E.P. 1976, The Study of Comets, ed. B. Donn et.al, NASA SP-393, pp. 334-356.
3. Noguchi, K., Sato, S., Maihara, T. & Okuda, H. 1974, Icarus 23, pp. 545-550.
4. Iijima, T., Matsumoto, T., Oishi, M., Okuda, H., & Ono, T. 1975, Publ. Astron. Soc. Japan 27, pp. 507-510.
5. Ney, E.P. & Merrill, K.M. 1976, Science 194, pp. 1051-1053.
6. Oishi, M., Kawara, K., Kobayashi, Y., Maihara, T., Noguchi, K., Okuda, H., & Sato, S. 1978, Publ. Astron. Soc. Japan 30, pp. 149-159.
7. Gebel, W.L. 1970, Astrophys. Jour. 161, pp. 765-777.
8. Stokes, G.M. 1972, Astrophys. Jour. 177, pp. 829-834.
9. Johnson, T.V., Lebofsky, L.A., & McCord, T.B. 1971, Publ. Astron. Soc. Pacific 83, pp. 93-94.
10. Babu, G.S.D. 1976, The Study of Comets, ed. B. Donn et.al, NASA SP 393, pp. 220-231.
11. A'Hearn, M.F., Millis, R.L., Birch, P.V. 1979, Astron. Jour. 84, pp. 570-579.
12. Liller, W. 1960, Astrophys. Jour. 132, pp. 867-882.
13. Donn, B., Powell, R.S. & Remy-Battiau, L. 1967, Nature 213, p. 379.
14. Giese, R.H. 1979, these proceedings, pp. 1.
15. O'Dell, C.R. 1971, Astrophys. Jour. 166 pp. 675-681.
16. Ney, E.P. 1974, Icarus 23, pp. 551-560.
17. Öhman, Y. 1941, Stock. Obs. Ann. Band 13, No. 11.
18. Blackwell, D.E. & Willstrop, R. V. 1957, Mon. Not. Roy. Astron. Soc. 117, pp. 590-599.
19. Oishi, M., Okuda, H. & Wickramasinghe, N.C. 1978, Publ. Astron. Soc. Japan 30, pp. 161-171.
20. Ono, T. 1976, Publ. Astron. Soc. Japan 28, pp. 229-238.
21. Clarke, D. 1971, Astron. & Astrophys. 14, pp. 90-94.
22. Isobe, S., Saito, K., Tomita, K. & Maehara, H. 1978, Publ. Astron. Soc. Japan 30, pp. 687-690.
23. Weinberg, J.L. & Beeson, D.E. 1976, Astron. & Astrophys. 48, pp. 151-153.
24. Weinberg, J.L. & Beeson, D.E. 1976, The Study of Comets, ed. B. Donn et. al, NASA SP-393, pp. 92-120.
25. Krishna Swamy, K.S. 1978, Astrophys. Space Sci. 57, pp. 491-497.
26. Becklin, E.E. & Westphal, J.A. 1966, Astrophys. Jour. 145, pp. 445-453.
27. Kleinmann, D.E., Lee, T., Low, F.J., & O'Dell, C.R. 1971, Astrophys. Jour. 165, pp. 633-636.
28. Maas, R.W., Ney, E.P., & Woolf, N.F. 1970, Astrophys. Jour. 160, pp. L101-L104.
29. Rieke, G.H., Low, F.J., Lee, T.A., & Wisniewski, W. 1975, Comet Kohoutek Workshop, ed. G.A. Gary, NASA SP-355, pp. 175-182.
30. Gatley, I., Becklin, E.E., Neugebauer, G., & Werner, M.W. 1974 Icarus 23, pp. 561-565.

31. Zeilik, M. & Wright, E.L. 1974, Icarus 23, pp. 577-579.
32. Merrill, K.M. 1974, Icarus 23, pp. 566-67.
33. Ney, E.P. 1975, Bull. Am. Astron. Soc. 7, p. 508.
34. Vanysek, V. & Wickramasinghe, N.C. 1975, Astrophys. Space Sci. 33,
      pp. L19.
35. Mendis, D.A. & Wickramasinghe, N.C. 1975, Astrophys. Space Sci,
      37, pp. L13-L16.
36. Brownlee, D.E. 1978, Cosmic Dust, ed. J.A.M. McDonnell, John Wiley,
      pp. 295-336.
37. Huffman, D.R., & Stapp, J.L. 1973, Interstellar Dust and Related
      Topics, ed. J.M. Greenberg & H. van de Hulst, pp. 297-301.
38. Krätschmer, W. & Huffman, D.R. 1979, Astrophys. Space Sci. 61,
      pp. 195-203.
39. Krätschmer, W. 1979, These proceedings, pp. 351.
40. Sekanina, Z. and Miller, F.D. 1973, Science 179, pp. 565-67.
41. Sekanina, Z. 1976, The Study of Comets, ed. B. Donn et. al, NASA
      SP-393, pp. 893-942.
42. Sekanina, Z. 1978, Astron. Astrophys. 68, pp. 429-435.
43. Sekanina, Z. 1979, these proceedings, p. 237.
44. Sekanina, Z. 1979, these proceedings, p. 251.
45. Labs, D. & Neckel, H. 1970, Solar Physics 15, pp. 79-87.
46. Mukai, T. 1977, Astron. Astrophys. 61, pp. 69-74.
47. Krishna Swamy, K.S. & Donn., B. 1979, Astron. Jour. 84, pp. 692-697.
48. Zaikowski, A. & Knacke, R.F. 1975, Astrophys. & Space Sci. 37,
      pp. 3-9.
49. Friedemann, C., Gürtler, J. & Dorschner, J. 1979, Astrophys. &
      Space Sci. 60, pp. 297-304.
50. Millman, P. 1976, Proc. IAU Colloq. 31, ed. H. Elsasser & H. Fech-
      tig, Lecture Notes in Physics 48, pp. 359-372.
51. Donn, B. 1977, Comets, Asteroids and Meteorites, ed. A.H. Delsemme,
      Univ. of Toledo, pp. 15-23.
52. Day, K.L. 1974, Astrophys. Jour. 192, pp. L15-L17.

DISCUSSION

Greenberg: You have so nicely summed up the present state of affairs
that your stated intent to raise questions has clearly succeeded. Many
questions occur to me, but let me raise just one. You showed that
comet polarization seems to be consistent with zodiacal light polar-
ization which is now attributed to complex large particles of various
sorts, yet the calculations on radiation pressure, temperature,
emission, etc. have so far been performed on individual spherical
particles. I wonder what the effect would be of considering complexes
of small particles. I can imagine that the emission of a relatively
large number of very small ($\leq .05\mu m$) silicate grains embedded in a
matrix of $\sim 50\mu m$ might well mimic some characteristics of an individual
larger ($> 1\mu m$) silicate particle. Perhaps one could consider a simpli-
fied radiation transfer problem to represent this effect. It should
be significant if the total optical depth at $10\mu m$ is > 1, which may just
be possible according to my calculations.

Hanner: Clearly, homogeneous spheres are a simplified case and there's much work to be done, both in the lab and theoretically. I'd like to see some measured optical constants for Don Brownlee's micrometeoroids. An approach to the radiation pressure for non-spherical particles is needed. Sekanina has shown that $\beta>1$ is required in some cases and fluffy particles seem like a good candidate. The detailed shape across the 10μm feature and the ratio of 10μm/18μm could be compared with the expectation for small embedded silicate grains.

Feldman: Is your model of the dust emission optically thin or thick and how does the derived spectrum at longer wavelengths compare with the data of Ney?

Hanner: The models I have shown here are optically thin. One needs particles a few microns or larger to explain a <u>blackbody</u> continuum at >10μm.

Lokanadham: Could this model explain the radio emission from cometary tails?

Hanner: I have not looked into the radio emission.

Fechtig: Is the formula which states that there is a cutoff in size really true or is it rather that one can not see the smaller particles? This can be the case particularly because of the bimodal character of the formula for β versus particle size.

Hanner: Some submicron grains may be present. From the optical data we can say only that they do not make a major contribution to the scattering or thermal emission.

Millman: In making model calculations, it is very important to remember the aggregate nature of most cosmic dust particles, extending down to submicron sizes, as revealed by collections made by Brownlee and others.